Proceedings of the Seventh International Conference on
Railway Technology: Research, Development and Maintenance
Edited by: J. Pombo
Civil-Comp Conferences, Volume 15, Paper 11.19
Civil-Comp Press, Edinburgh, United Kingdom, 2026
ISSN: 2753-3239, doi: 10.4203/ccc.15.11.19

Research on Vertical Vibration Characteristics and Vibration Suppression of HTS Maglev Dynamic Test Platform

Y. He[1], L. Wang[2], M. Wang[3], Y. Tan[3] and Z. Deng[4]

[1]School of Information Science and Technology, Southwest Jiaotong University, Chengdu, China
[2]Research Center for Super-High-Speed Evacuated Tube Maglev Transport, Southwest Jiaotong University, Chengdu, China
[3]State Key Laboratory of Rail Transit Vehicle System, Southwest Jiaotong University, Chengdu, China
[4]Research Center for Super-High-Speed Evacuated Tube Maglev Transport, Southwest Jiaotong University, Chengdu , China

Abstract

High-temperature superconducting (HTS) maglev features distinctive merits including friction-free operation, passive self-stabilization and zero inherent forward magnetic drag, rendering it a promising technical solution for future medium-and high-speed maglev transit. Under steady cruising conditions, irregularities on the permanent magnet guideway (PMG) induce vertical vibration and levitation gap fluctuation of the maglev system, which severely impairs vehicle operational stability. To investigate the vertical dynamic performance of the system, a launch test with a target speed of 45 m/s are conducted on the HTS maglev high-speed test platform, and the vibration response characteristics under steady cruising condition are analysed based on the test results. Based on the vibration characteristics, this paper proposes a non-contact vertical vibration suppression method using electromagnetic shunt dampers (EMSDs). The damping performance is verified through equivalent experiments, and further high-speed simulation validation is conducted using the validated dynamic model. This work systematically analyses the vertical dynamic performance of the HTS maglev system and quantitatively evaluates the vibration suppression effect of the proposed scheme, providing a valuable technical reference for the high-speed application of HTS maglev systems.

Keywords: maglev, dynamics, high-temperature superconducting, vibration suppression, electromagnetic shunt damper, test platform.

1 Introduction

With the continuous development of global rail transit industry, high-speed railway systems have attracted extensive attention from countries worldwide for their remarkable transport efficiency and prominent comprehensive economic benefits. As an emerging rail transit mode, high-speed maglev trains boast inherent advantages including no mechanical friction, excellent grade-climbing capacity and environment-friendly operation, and are widely recognized as a vital technical direction for the future development of rail transit.

Mainstream maglev technologies can be generally divided into three types, namely electromagnetic suspension, electrodynamic suspension and high-temperature superconducting (HTS) maglev [1], [2], [3]. Compared with other maglev technical schemes, HTS maglev is achieved through the interaction between high-temperature superconductors placed in levitators and a permanent magnetic guideway (PMG) [4], [5], [6], which possesses distinctive passive self-stabilization performance and zero intrinsic longitudinal magnetic drag, which render it highly suitable for medium-high-speed transit applications [7].

In 2000, China successfully rolled out the world's first manned HTS maglev vehicle [8]. Driven by this milestone, research teams globally have developed a variety of HTS maglev prototype vehicles in the subsequent years. A landmark technical leap was achieved in 2021 with the completion of the world's first engineering-oriented HTS maglev prototype, marking a substantial breakthrough in the industrialization progress of HTS maglev technology [9], [10], [11].

However, when vehicles run under steady cruising conditions, tiny geometric irregularities on the PMG will serve as continuous vertical excitations [12]. Such excitations easily trigger sustained vertical vibration and severe fluctuation of the levitation gap, which greatly degrade riding comfort and the long-term service reliability of the suspension system. Existing relevant researches mainly rely on numerical simulation or static bench tests to analyse maglev vibration responses, while few studies adopt scaled dynamic test platforms to capture real dynamic characteristics. Moreover, most existing vibration suppression measures rely on contact actuators, which introduce additional mechanical friction and limit the inherent advantages of friction-free maglev systems.

Against this background, this paper first conducts launch tests with a target speed of 45 m/s on the HTS maglev high-speed test platform to drive the proportional vehicle, and analyses the vertical vibration characteristics of the levitation system focusing on its constant-speed operation phase. A contactless vibration suppression scheme based on electromagnetic shunt dampers (EMSDs) is proposed accordingly. The vertical dynamic behaviours and damping performance are comprehensively explored by combining measured data and high-speed numerical simulations.

2 HTS Maglev Dynamic Model Test

Accurate characterization of dynamic behaviours is essential for the engineering application of HTS maglev systems, and reduced-scale moving model tests serve as a reliable experimental approach for this purpose. This section presents the dynamic model test of the HTS maglev proportional vehicle, providing experimental basis for subsequent dynamic modelling and vibration suppression study.

2.1 High-speed test platform

To promote the practical application of HTS maglev in future high-speed rail transit, it is essential to investigate its dynamic response characteristics under high-speed operating conditions. At present, numerical results obtained solely from dynamic simulation software cannot accurately reflect the influence of various practical factors on the dynamic responses of HTS maglev vehicles. Existing moving-test platforms such as SCML-03 [13] struggle to reproduce the genuine dynamic characteristics of the levitation system. In addition, the rotational operation mode of circular test tracks fails to precisely simulate the irregularity excitation of actual PMGs.

Therefore, conducting high-speed tests on a scaled dynamic test platform represents a more reasonable and effective approach. By employing a scaled HTS maglev vehicle model, this test platform can more accurately reproduce the real dynamic responses of HTS maglev systems during high-speed operation.

The high-speed HTS maglev test platform shown in Figure 1 mainly consists of three subsystems: (i) Levitation system including the PMG and the maglev scaled vehicle; (ii) Linear propulsion system that mainly composed of the power supply system, control system, and mover and stator of the linear motor; (iii) Permanent magnet eddy current braking system which adopts a permanent magnet array to realize contactless braking.

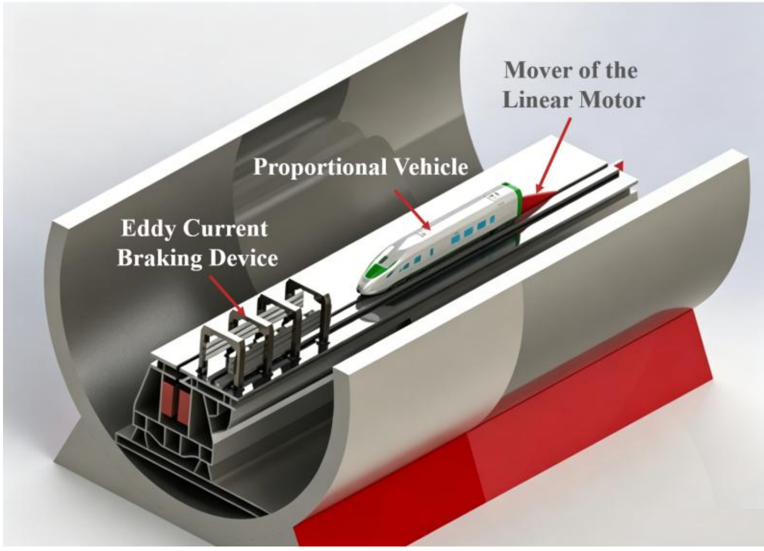

Figure 1: Overall composition diagram of the HTS maglev high-speed test platform.

2.2 Dynamic Model Test

A flywheel energy storage unit is employed in the test rig to provide ejection power [14]. The traction force is transmitted through the mechanical contact between the linear motor mover and the vehicle body. When the mover decelerates, the vehicle detaches and glides freely by inertia. Upon entering the braking section, the permanent magnet array of the eddy current brake interacts with the aluminium alloy shell of the scaled vehicle to generate braking force. The test platform and experimental equipment are shown in Figure 2. A high-precision linear encoder is arranged along the guideway to acquire real-time velocity and position signals of the proportional vehicle. In this paper, the operating condition with a target speed of 45 m/s is adopted for the analysis of vertical vibration characteristics.

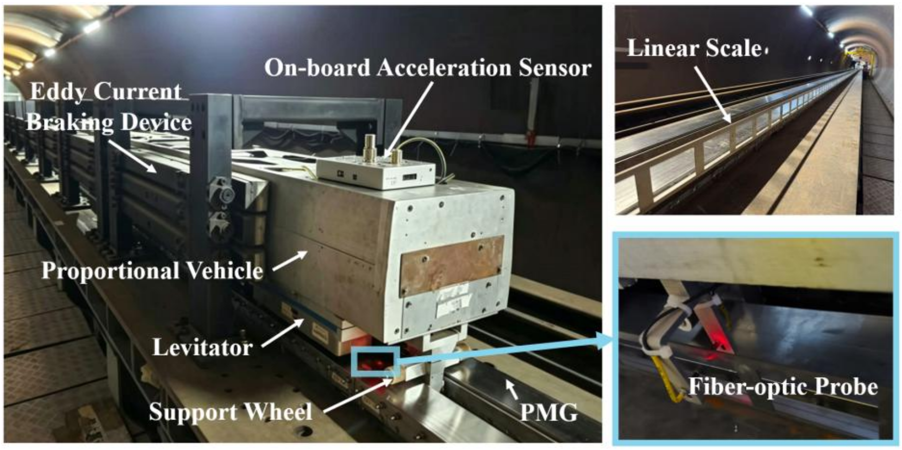

Figure 2: Test platform and experimental equipment.

Figure 3 shows the time-domain curves of operating speed and vertical vibration acceleration for the HTS maglev scaled vehicle during the whole test, with the shaded constant-speed cruising section selected as the core analysis interval. The test covers three typical phases: acceleration driven by the linear motor, free inertial gliding at steady speed, and deceleration to standstill via eddy current braking. Compared with the acceleration phase restricted by traction contact, the constant-speed section under fully free suspension exhibits significantly enhanced periodic vertical vibration induced by permanent magnet guideway irregularities. Such steady-state data free of external mechanical interference provides a reliable basis for subsequent dynamic model verification and vibration suppression analysis.

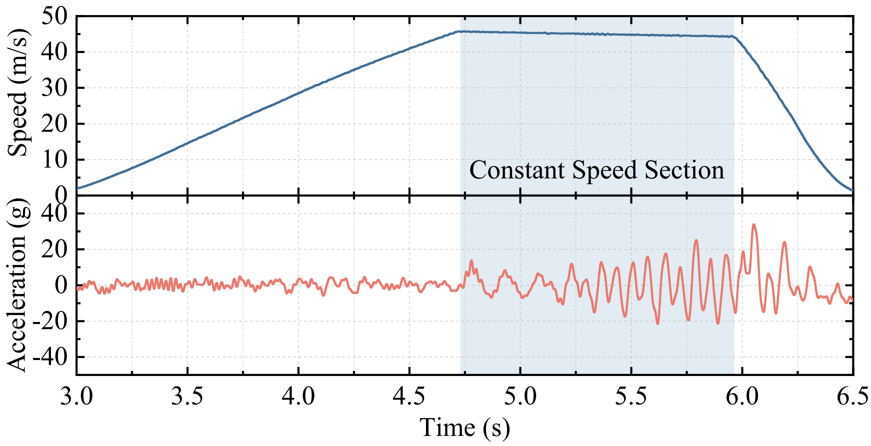

Figure 3: Experimental results of velocity and vertical acceleration.

3 Dynamic Modelling of HTS Maglev Proportional Vehicle

A reliable dynamic model is fundamental for analysing vibration characteristics and evaluating damping performance of HTS maglev systems. In this section, a dynamic model of the HTS maglev proportional vehicle is established and validated against test data, providing a numerical basis for subsequent vibration suppression research.

3.1 Vertical-Lateral Coupling HTS-PMG Relationship

The HTS-PMG relationship refers to the electromagnetic interaction between the high-temperature superconductor and PMG, that is acritical component of the HTS vehicle dynamic model. The levitation and guidance force characteristics of the HTS levitation unit are adopted from the static experimental measurements in reference [14], which serve as the fundamental data for the force model fitting in this work. In the test, a single levitator separated from the scaled maglev vehicle underwent vertical and lateral reciprocating motions, while force and laser displacement sensors captured force and displacement data.

The field cooling height (FCH) is set to 20 mm, and the levitation gap is fixed at 10 mm during the guidance force measurement. After two reciprocating cycles, the force-displacement hysteresis curves tend to be stable, and the test results are presented in Figure 4. The formula describing the HTS-PMG coupling relationship fitted from experimental data is shown in Equation 1 and 2, where z is the levitation height (m); y is the nominal lateral gap (m); The other parameters are used to adjust the levitation force and guidance force, and the relevant parameters are listed in Table 1.

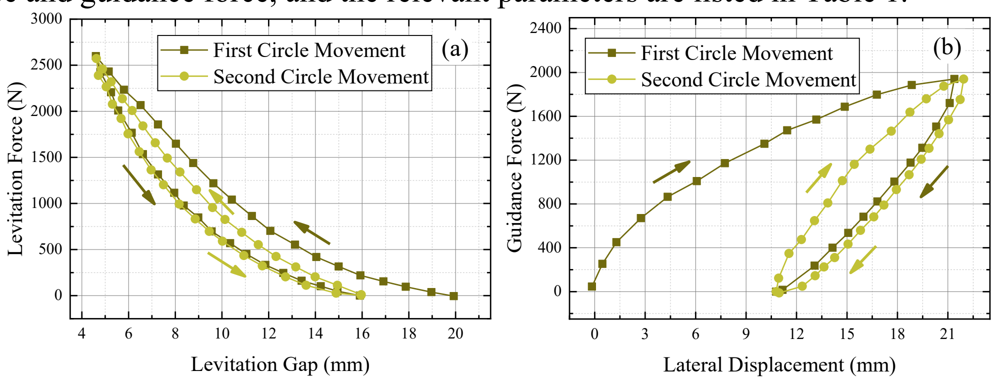

Figure 4: Measurement data of (a) Levitation force and (b) Guidance force [14].

$$F_{\text{lev}} = a_1\left(z-n_1\right)+b_1\left(z-n_1\right)^2+e_1 y+p_1 y^2+q_1\dot{z}+u_1 \tag{1}$$

$$F_{\text{gui}} = a_2\sin\left(q_2 y\right)\left(b_2\left(z-n_2\right)^2+u_2\left(z-n_2\right)+p_2\right)+e_2\dot{y} \tag{2}$$

Parameter	Value	Parameter	Value
a_1	-4.08×10^5	a_2	-1.29×10^6
n_1	0.0109	q_2	0.063
b_1	3.64×10^7	b_2	7260
e_1	1.21×10^4	n_2	0.01
p_1	4.6×10^6	u_2	-118
q_1	131	p_2	1
u_1	1180	e_2	228

Table 1: Parameters of levitation and guidance forces.

3.2 Simulation Modelling and Validation

The HTS maglev proportional vehicle is composed of a monolithic car body, with four levitators rigidly fixed at the four corners of its underside. Each levitator undergoes electromagnetic interaction with the PMG, producing both levitation force and guidance force to realize passive self-stabilizing levitation of the system.

Given the rigid consolidation between the car body and levitators without extra secondary suspension components, the vehicle is simplified as a single rigid body in dynamic modelling. The PMG irregularity is adopted as the primary external excitation for the system's dynamic response. The irregularity samples in this work are sourced from [15], which are illustrated in Figure 5.

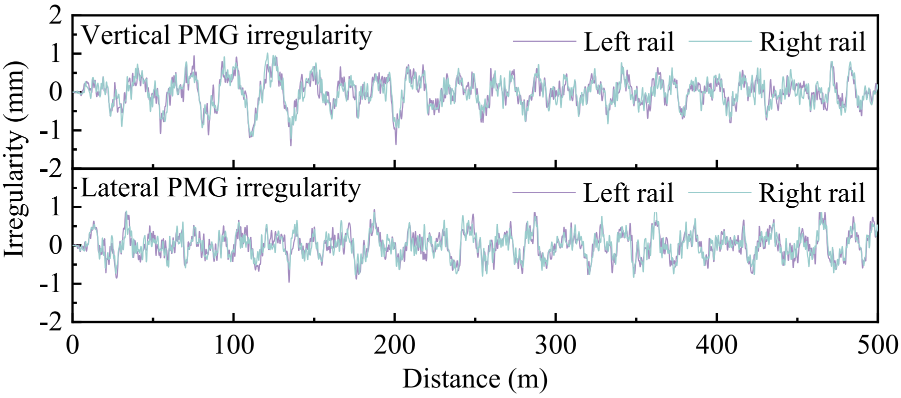

Figure 5: Samples of PMG irregularity.

To avoid spectral line, overlap and peak position misjudgement caused by insufficient frequency resolution due to the short acquisition duration of the constant-speed experimental segment, a simulation under the 45 m/s constant-speed condition is conducted with a duration of 10 s, referring to the actual length of the test track.

Figure 6 presents the frequency spectra of vertical acceleration from both simulation and experiment under the 45 m/s condition. The vibration characteristics show good consistency between simulation and test, with frequency errors of 0.833 Hz in the low-frequency band and 0.649 Hz in the mid-frequency band, respectively. Such favourable agreement verifies the accuracy of the established dynamic model, which can provide a reliable basis for subsequent research.

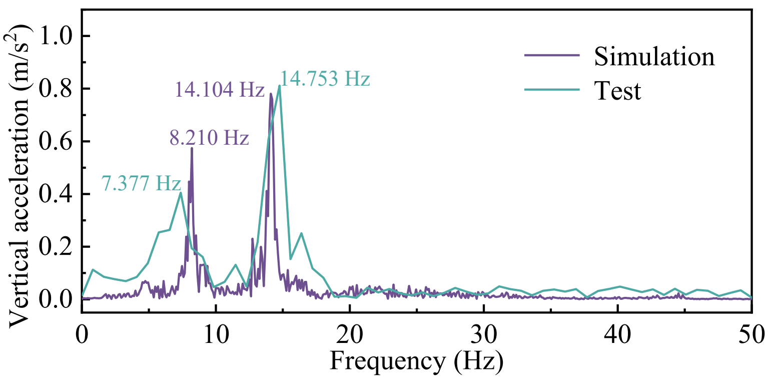

Figure 6: Frequency-domain comparison of vertical acceleration between dynamic model test and simulation.

4 Vibration Suppression Scheme and Performance Verification

Given the remarkable vertical vibration of the HTS maglev system, a non-contact vibration suppression scheme using EMSDs is investigated in this chapter. The damping performance of the scheme is verified through equivalent bench tests and high-speed co-simulation, providing a technical reference for vibration control design of high-speed HTS maglev vehicles.

4.1 Equivalent Vibration Suppression Test of the EMSD

The foregoing dynamic characteristic analysis and model verification demonstrate that the scaled HTS maglev vehicle exhibits remarkable vertical vibration under the 45 m/s constant-speed cruising condition. Excessive vibration will not only deteriorate the levitation stability of the system, but also adversely affect the long-term service reliability of the superconducting levitation units. To mitigate this problem, this work applies an EMSD to suppress the system vibration.

EMSD is a non-contact vibration suppression device, recognized as one of the most effective damping solutions for HTS maglev bearings and maglev vehicles [16], [17]. As depicted in Figure 7, it generally consists of permanent magnets, electromagnetic coils, and an external shunt impedance circuit. Relative motion between the closed coil and the magnet induces electromotive force and induced current, which interacts with the magnetic field to resist relative motion and achieve damping; the damping performance is closely determined by the shunt impedance circuit parameters.

Benefiting from its non-contact working mode, EMSD fits the demand of levitation systems. Its effective stroke matches the millimetre-level vibration amplitude typical of HTS maglev systems, and the inherent permanent magnet guideway in the levitation system eliminates the need for additional excitation devices. Therefore, EMSD presents high compatibility with HTS maglev application scenarios.

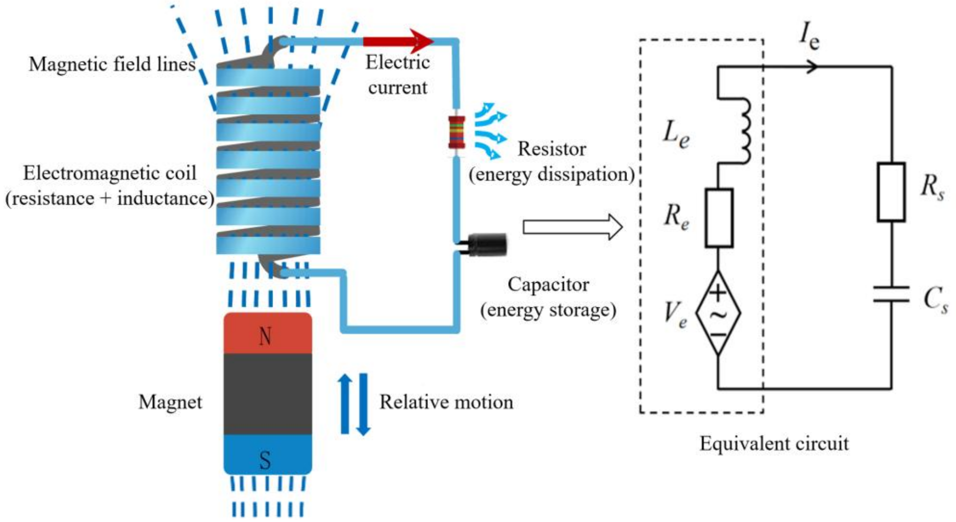

Figure 7: Schematic diagram of the EMSD.

Equivalent experimental tests are first conducted to verify the vibration suppression effect of the proposed scheme. The experimental equipment is shown in Figure 8. First, free vibration tests are conducted. Liquid nitrogen is continuously fed into the test levitator to cool the HTS bulks down to the superconducting state. Once stable

levitation is achieved, vertical free vibration is excited by tapping the center of the levitator's top surface. The measured vertical natural frequency of the levitator is approximately 7.45 Hz, and a slight increase in vibration response appears at 14.66 Hz, corresponding to the second harmonic of the system, as depicted in Figure 9.
The above main frequency and harmonic characteristics are highly consistent with the frequency-domain results of the dynamic model test. This consistency verifies that the inherent dynamic properties of the bench levitation system match the dominant vibration characteristics under dynamic model operating conditions. Accordingly, this test bench can be adopted to perform equivalent excitation tests for evaluating the vibration suppression performance of the EMSD.

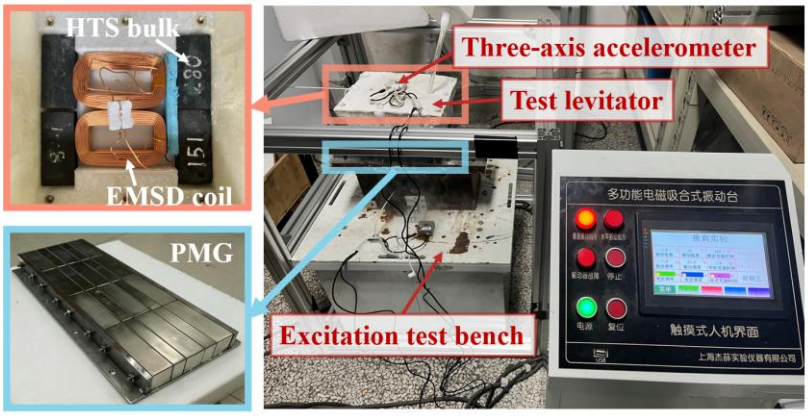

Figure 8: Experimental equipment of vibration test.

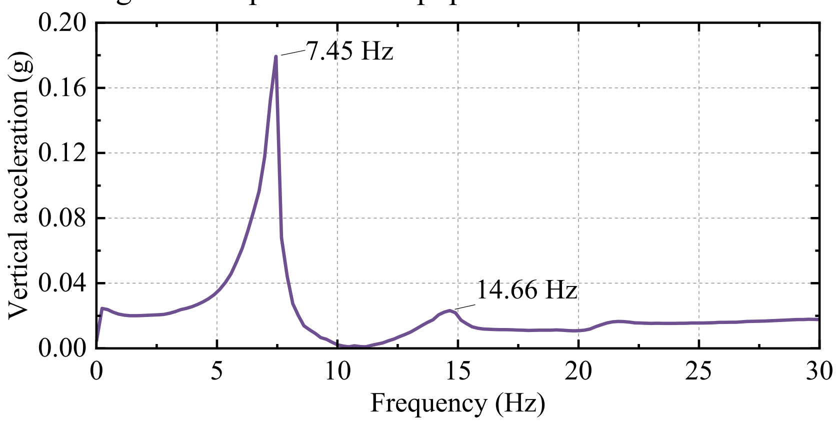

Figure 9: Frequency spectrum of vertical free vibration of the levitator.

Subsequently, excitation tests are conducted. The vertical excitation frequency of the vibration bench is swept from 5 Hz to 20 Hz with a step size of 1 Hz. The EMSDs are switched between deactivated and activated states by setting the coil circuit to open-circuit and closed-circuit respectively. Acceleration signals are acquired via a data acquisition system, and the root-mean-square (RMS) values of vibration acceleration are derived from the measured data.
As shown in Figure 10, the vertical vibration of the system shows two peaks at 8 Hz and 17 Hz without EMSD, with the maximum amplitude of 6.497 m/s^2 occurring at 8 Hz. When the EMSD is in operation, the vibration peaks are located at 8 Hz and 16

Hz, and the peak value reaches 2.83 m/s² at 16 Hz. At the excitation frequency of 8 Hz, the RMS value of vibration acceleration drops to 2.561 m/s². The EMSD significantly attenuates the vibration response in the resonance frequency band, exhibiting favourable vibration suppression performance.

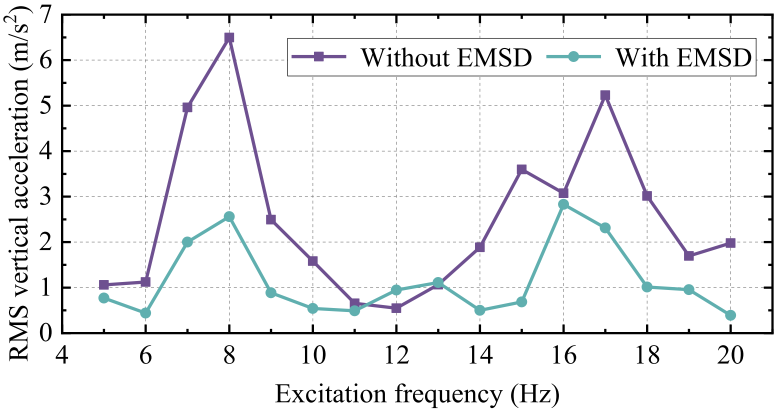

Figure 10: Vertical dynamic response of the levitator under forced vibration.

4.2 Verification of Vibration Suppression via High-speed Simulation

To systematically investigate the vibration suppression performance of the EMSD under high-speed operating scenarios, this section carries out co-simulation calculations for two typical high-speed conditions of 400 km/h and 500 km/h based on the validated HTS dynamic model presented in Section 3.2. The EMSD coils are arranged at the four levitators, with their bottom surfaces flush with the levitators, as shown in Figure 11.

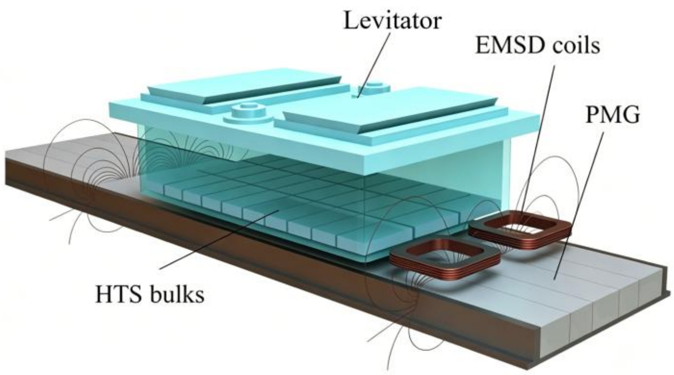

Figure 11: Mechanical and circuit models of HTS maglev system with EMSD.

The EMSD model is established in Simulink, as illustrated in Figure 12. Where z is the vertical displacement of levitators relative to PMG; i is the current in the circuit, L is inductance and R is the total resistance of EMSD system, k_v is called the electromechanical coupling factor, f_m denotes the Lorentz damping force generated to suppress coil vibration when the coil oscillates within a gradient magnetic field.

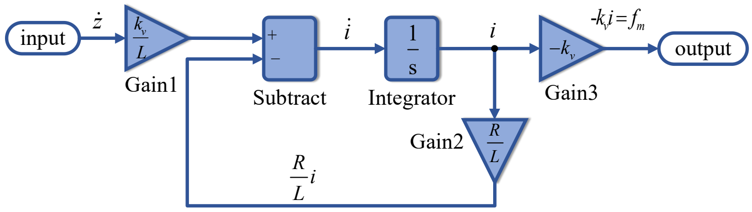

Figure 12: Control block diagram of EMSD in Simulink control module.

Figure 13 illustrates the main workflow of the co-simulation. The real-time dynamic response of the vehicle calculated by the Universal Mechanism model serves as the input to the Simulink control model, and the damping force computed via Simulink is fed back into Universal Mechanism to form a closed-loop simulation. This framework can effectively characterize the operating dynamics of the system under the action of the EMSD.

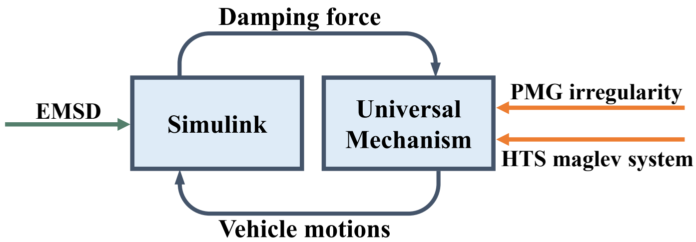

Figure 13: Schematic diagram of co-simulation.

Figure 14 depicts the frequency-domain characteristics of vertical acceleration of the levitation system with and without the EMSD at the two speeds. It is observed that the EMSD delivers remarkable suppression effect on the vertical main resonance of the superconducting maglev system. Notably, the vibration response with the EMSD exhibits a slight rise in the high-frequency band, which arises from the circuit resonant frequency introduced by the EMSD that alters the harmonic characteristics of the system to a certain extent.

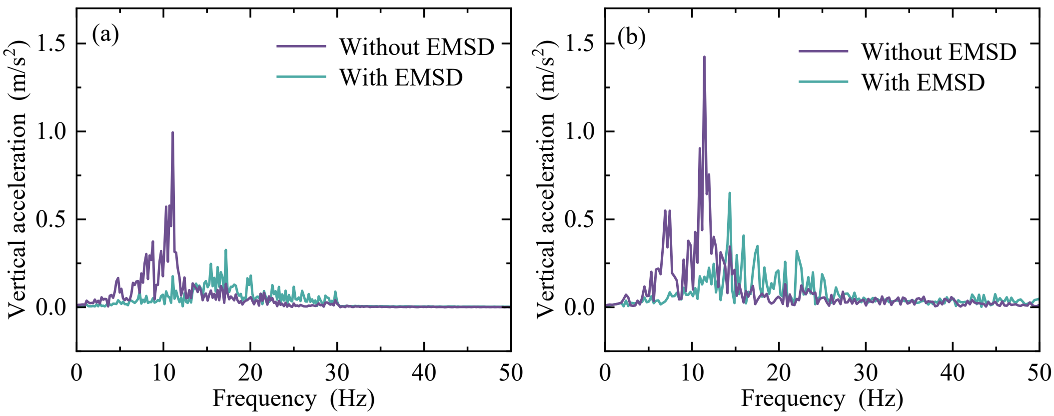

Figure 14: Simulation results of vibration suppression. (a) 400 km/h; (b) 500 km/h.

Comparison across different speed conditions shows that the overall vibration amplitude of the system increases with rising travel speed, yet the vibration suppression rule of the EMSD remains stable. The above simulation results verify that the EMSD can effectively dissipate vibration energy in the main frequency band and suppress vertical main resonance over a wide frequency range, and possesses favourable engineering application value for improving the operational stability of high-speed maglev vehicles.

5 Conclusions

Based on the HTS maglev high-speed test platform, this paper investigates the vertical vibration characteristics of the levitation system and proposes a non-contact vibration suppression scheme with EMSD. The test under 45 m/s are carried out to capture the vertical vibration response induced by PMG irregularities on excitations, and the damping performance of the proposed scheme is systematically verified through experimental measurements and high-speed numerical simulations.

The results indicate that the EMSD can effectively dissipate vibration energy and significantly reduce the amplitude of the main vertical resonance peak, and its damping effect is fully validated under the test speed condition. When extended to high-speed scenarios of 400 km/h and 500 km/h, the EMSD still maintains reliable vibration suppression performance, showing satisfactory adaptability over a wide speed range. The slight rise in the high-frequency band, which arises from the circuit resonant frequency introduced by the EMSD that alters the harmonic characteristics of the system to a certain extent.

Benefiting from the inherent merits of friction-free operation, passive self-stabilization and zero inherent forward magnetic drag, HTS maglev has become a highly promising technical route for future high-speed rail transit. The vibration control method proposed in this paper effectively improves the operational stability of the levitation system under high-speed conditions, further verifies the application feasibility of HTS maglev in medium-high-speed and ultra-high-speed scenarios, and provides a valuable reference for the subsequent engineering development of this technology.

References

[1] P. Holmer, “Faster than a speeding bullet train,” *IEEE Spectr.*, vol. 40, no. 8, pp. 30–34, Aug. 2003.

[2] S. Ohtani, O. Hosokawa, and A. Siraki, “Design of the linimo maglev train,” *IATSS Rev.*, vol. 32, pp. 14–20, 2007.

[3] K. Sawada, “Outlook of the superconducting maglev,” *Proc. IEEE*, vol.97, no. 11, pp. 1881–1885, Nov. 2009.

[4] Z. Deng et al., “Ahigh-temperature superconducting Maglev ring test line developed in Chengdu, China,” *IEEE Trans. Appl. Supercond.*, vol. 26, no. 6, Sep. 2016, Art. no. 3602408.

[5] R. M. Stephan and A. O. Pereira, “The vital contribution of Maglev vehicles for the mobility in smart cities,” *Electronics*, vol. 9, no. 6, pp. 978–999, Jun. 2020.

[6] G. Lanzara and G. D’Ovidio, “Characterization method of the V-shaped high-temperature superconducting Maglev module for transport system applications,” *J. Supercond. Novel Magn.*, vol. 35, no. 5, pp. 1071–1078, Feb. 2022.

[7] Z. Deng, L. Wang, H. Li, J. Li, H. Wang, and J. Yu, “Dynamic studies of the HTS maglev transit system,” *IEEE Trans. Appl. Supercond.*, vol. 31, no. 5, Aug. 2021, Art. no. 3600805.

[8] J. Wang et al., “The first man-loading high temperature superconducting maglev test vehicle in the world,” *Physica C-Supercond. Appl.*, vol. 378, pp. 809–814, Oct. 2002

[9] G. D’Ovidio, F. Crisi, and G. Lanzara, “Design and optimization of UAQ4 experimental maglev module,” *Materials Sci. Forum.*, vol. 670, pp. 42–47, 2011.

[10] F. Hellman, E. M. Gyorgy, D. W. Johnson, H. M. Obryan, and R. C. Sherwood, “Levitation of a magnet over a flat type II superconductor,” *J. Appl. Phys.*, vol. 63, no. 2, pp. 447–450, 1988.

[11] L. Schultz et al., “Superconductively levitated transport system- The SupraTrans project,” *IEEE Trans. Appl. Supercond.*, vol. 15, no. 2, pp. 2301–2305, Jun. 2005.

[12] X. Zhou et al., “Analysis of the influence of EMD-based irregularity components on the vibration response of the HTS pinning Maglev vehicle under high-speed operation,” *J.Vib.Eng.Technol.*, vol.13, no.8, Oct. 2025, Art. no. 542.

[13] J. Wang et al., “A high-temperature superconducting Maglev dynamic measurement system,” *IEEE Trans. Appl. Supercond.*, vol. 18, no. 2, pp. 791–794, Jun. 2008.

[14] Z. Deng et al., “A high-speed running test platform for high-temperature superconducting maglev,” *IEEE Trans. Appl. Supercond.*, vol. 32, no. 4, Jun. 2022, Art no. 3600905.

[15] Y. Yuan et al., “On-board and inverse reconstruction measurement method for PMG irregularity measurement of HTS pinning maglev,” *Measurement*, vol. 273, May 2026, Art no. 121182.

[16] Y. Huang et al., “multi-objective parameter optimization of electromagnetic shunt damper for high-temperature superconducting Maglev vehicle system,” *J. Vib. Control*, vol. 30, no. 17/18, pp. 4118–4130, Sep. 2024.

[17] H. Li et al., “Enhancing lateral dynamic performance of HTS Maglev vehicles using electromagnetic shunt dampers: Optimisation and experimental validation,” *Veh. Syst. Dyn.*, May 2025, doi: 10.1080/00423114.2025.2510533.